

First Passage Times and Time-Temperature-Transformation curves for Martensites

Madan Rao¹ and Surajit Sengupta²¹Institute of Mathematical Sciences, Taramani, Madras 600113, India²Material Science Division, Indira Gandhi Centre for Atomic Research, Kalpakkam 603102, India

(April 15, 2024)

Martensites are long-lived nonequilibrium structures produced following a quench across a solid state structural transition. In a recent paper (Phys. Rev. Lett. 78, 2168 (1997)), we had described a mode-coupling theory for the morphology and nucleation kinetics of the equilibrium ferrite phase and twinned martensites. Here we calculate nucleation rates within a first-passage time formalism, and derive the time-temperature-transformation (TTT) diagram of the ferrite-martensite system for athermal and isothermal martensites. Empirically obtained TTT curves are extensively used by metallurgists to design heat treatment cycles in real materials.

PACS: 81.30.Kf, 81.30.-t, 64.70.Kb, 64.60.Qb, 63.75.+z

A martensitic transformation [1] is a nonequilibrium solid state structural transition which results in a metastable phase (martensite), often consisting of alternating twinned arrays within the parent solid (austenite). A characteristic of this transformation is that it is diffusionless, i.e., the velocity of the transformation front is much larger than typical diffusional speeds of atoms. In contrast, in nitidamente slow cooling results in the equilibrium phase (ferrite).

Martensites are commercially important, for example as the hard constituent in steel, or in shape-memory alloys like Nitinol. These desirable properties, depend on the amount of transformed martensite. Over the years a tremendous amount of empirical [1] and theoretical [2,3] knowledge regarding the kinetics of this transformation has accrued. A convenient representation, used extensively by metallurgists is the time-temperature-transformation diagram [4]. The TTT diagram (Fig. 1), is a family of curves parametrized by the fraction

of transformed product. Each curve is a plot of the time required to obtain versus temperature of quench. It is clear from the figure that the shape of the curves are qualitatively different for the ferrite and martensite products. There are two important features regarding the TTT curves for martensites. (i) The transformation curves lie below a temperature M_s , the martensite-start temperature. This means that a martensite does not obtain at temperatures above M_s , even if the quench rates are infinitely high. (ii) The curves are parallel to the time axis. This implies that the martensitic transformation is completed immediately following the quench (such martensites are called athermal martensites). Such transformation curves have been obtained empirically; in the

absence of a unified nonequilibrium theory for martensite and ferrite nucleation, these curves have not been derived.

In a recent paper [5] we presented a mode-coupling theory for the nucleation and growth of a product crystalline droplet within a parent crystal. We showed that for slow quenches, the droplet grows diffusively as an equilibrium ferrite inclusion, while for fast quenches, the droplet grows ballistically, as a martensite having twinned internal substructure, with a speed comparable to the sound velocity. Given this unified description, can we arrive at the general features of the phenomenologically obtained TTT curves? The details of the underlying physics are of course complex — this includes an understanding of the heterogeneous nucleation and growth of martensitic grains and other intervening phases, and the subsequent collision of grains emanating from correlated nucleation events. In this Letter, we demonstrate that certain qualitative aspects of the TTT diagram can nevertheless be obtained using very general features of the distribution of nucleation events and the nucleation dynamics arising from our mode-coupling theory [5].

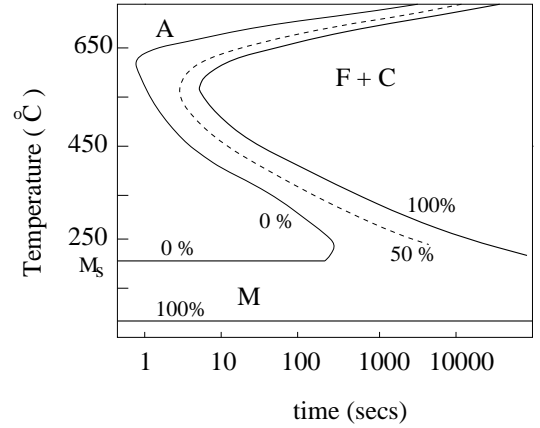


Fig. 1 Experimental TTT curves (adapted from Ref. [4]) for the structural steel A ISI 1090, containing approximately 0.84% C and 0.60% Mn. The letters A, F and C represent the f.c.c.-austenite, the equilibrium b.c.c.-ferrite and the carbide precipitate (Fe_3C) respectively. Curves corresponding to 0, 50 and 100 % transformation are shown. Below a temperature M_s , the metastable martensite (M) is formed — the transformation curves for martensites are horizontal.

Though our analysis can be generalized to any structural transition in arbitrary dimensions, we will, for calculational simplicity, focus on the square to rhombus structural transition in 2-dimensions. It will be clear that the qualitative form of the leading 'edge' of the TTT curves (labelled 0% in Fig. 1) is independent of dimensionality and the type of structural transition.

The square to rhombus structural transformation involves a shear+volume deformation, and so the strain order parameter ϵ_{ij} has only one nontrivial component $\epsilon_{12} = (\partial_y u_x + \partial_x u_y)/2$ (u is the displacement field). A quench across this transition results in the nucleation of a rhombic product in a square parent. At the initial time, the transformed region is simply obtained as a geometrical deformation of the parent creating a local atomic mismatch [1]. This leads to a discontinuity in the normal component of the displacement field across the parent-product interface $u \cdot \hat{n}$ (\hat{n} is the unit normal to the interface) [6]. This discontinuity appears as the vacancy field $(\partial_{\hat{n}} n_{\text{vac}}) = n$, where δ is the interfacial thickness, n is the average number density, and n_{int} and n_{vac} are the interstitial and vacancy densities respectively (measure of the compression or dilation of the local atomic environment) [7].

The free-energy functional F describing this inhomogeneous configuration contains the usual bulk elastic free-energy of a solid F_{el} and an extra interfacial term describing the parent-product interface [5]. In our 2-d example, the bulk free energy F_{el} is constructed to have three minima $\epsilon_{12} = 0$ (one corresponding to the undeformed square cell ($\epsilon = 0$)) and the other two corresponding to the two variants of the rhombic cell ($\epsilon = \pm \epsilon_0$). The total (dimensionless) free-energy functional to leading order in ϵ is,

$$F = \int_{\text{area}} \left[\frac{1}{2} a^2 \epsilon^2 + \frac{1}{2} b^2 \epsilon^2 + \frac{1}{2} (c(r) \epsilon)^2 \right] : \quad (1)$$

The modulus $c(r) = \frac{1}{2} P_0 \partial_n \partial_n c(r)$ (prime denotes a sum across the interface) is the surface compressibility of the vacancy field and depends on the local orientation of the parent-product interface ($c(r)$ is the direct correlation function of the liquid at freezing). The three minima of the homogeneous part of F at $\epsilon = 0$ (square) and $\epsilon = \pm \epsilon_0 = [(1 + \frac{1}{2} - 3a)/3]^{1/2}$ (rhombus), are obtained in the parameter range $0 < a < 1/3$. The first-order structural transition from the square to rhombus occurs at $a = 1/4$. For $1/4 > a > 0$, the square is metastable. The degree of undercooling $1/4 - a / T_s$, where T_s is the temperature at which the equilibrium structural transition occurs.

A quench across the structural transition, nucleates a region of the product ($\epsilon = \pm \epsilon_0$) within the parent ($\epsilon = 0$). The growth of this nucleus is described by a Langevin equation for the broken symmetry variable ϵ and the vacancy field n . Moving with the growing interface, the equations of motion become,

$$\frac{\partial \epsilon}{\partial t} = -\frac{F}{\epsilon} + \xi \quad (2)$$

$$\frac{\partial n}{\partial t} = D \nabla^2 n - \frac{F}{n} : \quad (3)$$

where the noise ξ is an uncorrelated gaussian white noise with variance proportional to temperature $\langle \xi(x;t) \xi(x';t') \rangle = 2k_B T \delta(x-x') \delta(t-t')$. D is the microscopic vacancy diffusion coefficient which has an Arrhenius dependence $D = D_1 \exp(-A/k_B T)$. Typical values of parameters for pure (99.98%) Fe at around 1223–1473 K have been measured to be $A = 280 - 310 \text{ kJ mol}^{-1}$ and $D_1 = 0.4 - 4.0 \text{ cm}^2/\text{s}$, which gives $D \approx 10^{12} \text{ cm}^2/\text{s}$.

Our free-energy functional naturally admits two widely separated time scales τ_1 , the relaxation time of the order parameter to the local minimum and τ_n , the first-passage time for the order parameter to go from the local to the global minimum. The shorter time scale $\tau_1 = [F''(\epsilon = 0)]^{-1/2} = \epsilon/c$ (c is the velocity of transverse sound) with a typical value of 10^{-14} s [9]. The relaxation time of n , given by $\tau_n = D/\epsilon^2$, lies between $\tau_1 < \tau_n$. Thus the order parameter is 'slaved' to n , which acts as a time dependent source coupling to ϵ . The 'instantaneous' value of ϵ is given by the Eq. (3).

The exact formula for the nucleation rate of a solid nucleus growing within a solid parent is unknown. In a continuum field theory approximation, the first passage time τ_n would be given by the Kramers formula with a time-dependent energy barrier [9]. In this paper we shall take $\tau_n = \tau_1 \exp(E)$, where E is the energy barrier (in units of $k_B T$) to form the critical nucleus. We have ignored the curvature dependent prefactors since they are only weakly dependent on $\epsilon(t)$ and a .

To calculate the energy of the critical nucleus, we use a variational ansatz for the strain profile defining a nucleus of linear dimension L ,

$$\epsilon(x;y) = \begin{cases} \epsilon_0 & \text{if } L/2 + \delta/2 < x < L/2 - \delta/2 \\ \text{and } L/2 + \delta/2 < y < L/2 - \delta/2 \\ 0 & \text{if } L/2 - \delta/2 > x > L/2 + \delta/2 \\ \text{or } L/2 - \delta/2 > y > L/2 + \delta/2 \end{cases} \quad (4)$$

Within the interface of width δ , the strain linearly interpolates between 0 and ϵ_0 (see Fig. 2(a)). The vacancy field $n(x;y;t)$ is obtained from a solution of the diffusion equation Eq. (3), with the initial condition that $n(x;y;0) = u \cdot \hat{n}$, where u can be computed from the variational ansatz Eq. (4);

$$n(x;y;t) = n(x;y-L/2;t) + n(y;x-L/2;t) + n(x;y+L/2;t) + n(y;x+L/2;t) \quad (5)$$

within the interface and 0 without, where

$$n(a;b;t) = \frac{1}{4 D t} \int_{L/2 - \delta/2}^{L/2 + \delta/2} dx \int_{L/2 - \delta/2}^{L/2 + \delta/2} dy \exp \left[-\frac{a(x')^2 + b(y')^2}{4 D t} \right] : \quad (6)$$

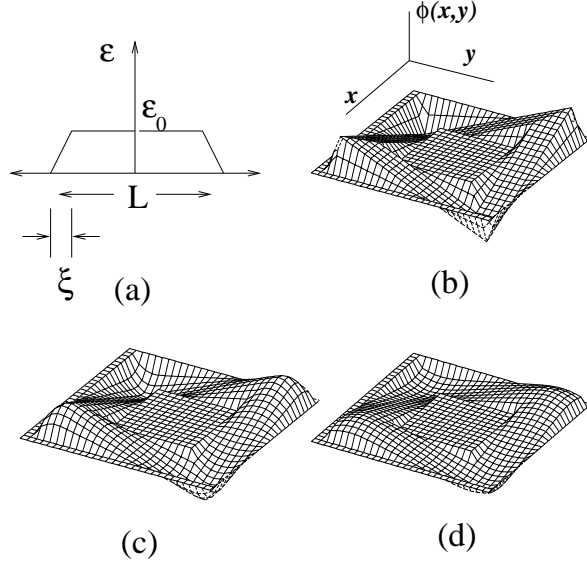


Fig. 2 (a) Variational ansatz for ϕ showing a cross-section across a square shaped nucleus of size L and interface width ξ . (b)-(d) 3-d plots showing a sequence of $\phi(x,y;t)$ surrounding the nucleus at different times.

Figures 2 (b)-(d) is a sequence of three-dimensional plots of $\phi(x,y;t)$ at different times. A positive (negative) ϕ indicates a higher interstitial (vacancy) density. The free-energy of a nucleus of size L at a given time t , $E(L;t)$, is obtained by substituting the variational form for ϕ and the 'field' $\phi(x,y;t)$ in Eq. (1). For every $L;t$, we minimize the energy $E(L;t)$ with respect to the variational parameter ϕ , to obtain $E(L;t)$. The energy E and size L of the critical nucleus for every time t , is determined by $dE(L;t)/dL|_{L=L_c} = 0$. The energy of the critical nucleus decreases with time, and so nucleation of the stable phase will occur when the time dependent nucleation barrier becomes small enough. This is obtained by self-consistently solving

$$n = \frac{1}{\Omega} \exp(-E(L_c;t)) : \quad (7)$$

Once the nucleus exceeds the critical size it grows. Thus the leading edge of the TTT curves, defined as the time required to form a certain amount of the product at a given temperature of quench, should be given by Eq. (7). This however does not take into account the rate at which nuclei are produced. There are principally two kinds of nucleation modes [10] — (i) Athermal and (ii) Isothermal. A number of alloys like the one portrayed in Fig. 1, follow the athermal mode of martensite production. The amount of martensite formed is a function only of the temperature of quench and not the time of holding at that temperature [11]. A convenient parametrisation is

$$\frac{dN(t)}{dt} = N_0(T) (1 - \exp(-t/t_0)) ; \quad (8)$$

where $t_0 \propto 1/n$ and $N_0(T)$ increases with decreasing T below M_s . It is clear that as long as $t_0 \propto 1/n$, all grains are essentially nucleated at once, and the leading edge of the TTT curves is given by n (solid line in Figure 3). The curves in Figure 3, have been derived using the quoted values for the parameters D_1 and A for Fe alloys [12]. The modulus is fixed by the condition that the intercept $a_{M_s}(t) = M_s = 4T_s$. For Fe alloys, $M_s = 100 - 200$ C and $T_s = 900$ C, leading to $a = 0.1$. The time axis is in units of t^{-1} taken to be 10^{-6} s. All these parameters can be varied over a wide range without changing the qualitative nature of the results.

For low undercooling (small $1=4/a$), the critical barrier height is large. The field relaxes quickly, and so n asymptotes the $D = 1$ curve (dotted line in Fig. 3). Once the critical nucleus is formed, it grows as a ferrite [5]. For larger undercooling, D decreases reaching a vanishingly small value for $a \rightarrow a_{M_s}$. This part of n (a) asymptotes the $D = 0$ curve, when the field remains frozen at the parent/product interface. As shown in Ref. [5], the nucleus twins in the direction of motion resulting in a martensite.

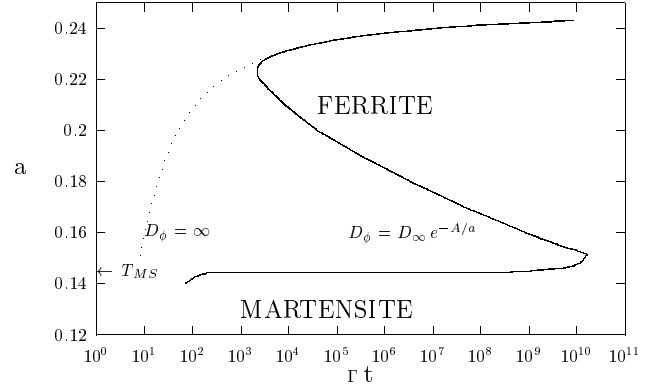


Fig. 3 Calculated leading edge of the TTT curves showing ferrite and athermal martensite regions (solid line). The values for D_1 and A in dimensionless units have been translated from the quoted values for Fe (see text) | $D_1 = 4 \cdot 10^{14}$ and $A = 8$. The arrow indicates the martensite-start temperature a_{M_s} in our units. The dashed curve shows the first passage time for $D = 1$.

Our calculation thus successfully reproduces the two distinctive features of athermal martensites — the horizontal martensite transformation curves, and a well defined martensite-start temperature M_s which is independent of D_1 and decreases with increasing a .

On the other hand in isothermal martensites, the nuclei are thermally generated, and so t_0 is large compared to n . In this situation, the leading edge of the TTT curve

does not have a precise meaning. We can nevertheless define the leading edge from the product $(dN/dt)_n^{-1}$. Being produced by a thermal activation process, dN/dt decreases with increased undercooling. However as stated above, the critical barrier height and hence n decreases with increased undercooling. This produces the characteristic C-shaped TTT curves of the isothermal martensite [10]. The qualitative features of the leading edge do not change if the isothermal nucleation is autocatalytic.

The other curves in the TTT family (Fig. 1) correspond to the transformation of a fixed amount of the product. This requires a detailed knowledge of the dynamics of patterning generated by the nucleation and growth of grains [13], together with the shape and size of the individual grains.

In summary, we have derived the essential features of the leading edge of the time-transformation-temperature curves for both athermal and isothermal martensites, within the first-passage time formalism. This makes use of a recently developed [5] mode-coupling theory for the morphology and nucleation kinetics of the equilibrium ferrite and twinned martensites. Such transformation curves have thus far been obtained empirically, and to the best of our knowledge have never been derived.

Most martensites contain alloying elements which occur as interstitial or substitutional impurities. The solubility of these impurities may be different in the parent and product phases (eg., interstitial carbon in steel). This would induce large scale diffusion of impurities as the transformation proceeds (eg., carbon diffuses away from the ferritic product). TTT diagrams of such alloy steels often show a secondary bulge together with the formation of an intermediate structure called bainite. These issues may be understood within our formalism by coupling the density of impurities to the strain. We investigate the role of alloying in a forthcoming publication.

We thank K. P. N. Murthy for a discussion on time-dependent nucleation barriers.

- [6] L. D. Landau and E. M. Lifshitz, in *Theory of Elasticity* (Pergamon Press, 1989).
- [7] The product might prefer to generate dislocations at the parent-product interface (producing internal slip bands).
- [8] Smithells Metals Reference Book, 7th edition, eds. E. A. Brandes and G. B. Brook (Butterworth-Heinemann, Oxford, 1992).
- [9] G. S. Agarwal and S. R. Shenoy, *Phys. Rev. A* **23**, 2719 (1981); S. Chandrasekhar in *Selected Papers on Noise and Stochastic Processes*, ed. N. Wax (Dover, NY, 1957).
- [10] V. Raghavan, in *Martensite*, eds. G. B. Olson and W. S. Owen (ASM International, The Materials Information Society, 1992).
- [11] The microscopic explanation of such a nucleation process is unclear, though some experiments (V. Raghavan and M. Cohen, *Acta Metall.*, **20**, 1251 (1972)) suggest a thermal origin.
- [12] The qualitative features of the leading edge of the TTT curves, depend only on gross features of the time dependence of the barrier height. In particular they are insensitive to the nature of the order parameter, dimensionality, shape of the nucleus etc. This aspect allows us to use the measured parameters for Fe alloys (a 3-dim FCC \rightarrow BCC transition) in our calculation.
- [13] M. Rao, S. Sengupta and H. K. Sahu, *Phys. Rev. Lett.* **75**, 2164 (1995); E. Ben-Naim and P. Krapivsky, *Phys. Rev. Lett.* **76**, 3234 (1996); M. Rao and S. Sengupta, *Phys. Rev. Lett.* **76**, 3235 (1996).

-
- [1] A. Roitburd, in *Solid State Physics*, ed. Seitz and Turnbull (Academic Press, NY, 1958); Z. Nishiyama, *Martensitic Transformation* (Academic Press, NY, 1978); A. G. Kachaturyan, *Theory of Structural Transformations in Solids* (Wiley, NY, 1983).
 - [2] G. R. Barsch and J. A. Krumhansl, *Phys. Rev. Lett.* **37**, 9328 (1974); G. R. Barsch, B. Horowitz and J. A. Krumhansl, *Phys. Rev. Lett.* **59**, 1251 (1987).
 - [3] G. S. Bales and R. J. Gooding, *Phys. Rev. Lett.* **67**, 3412 (1991); A. C. E. Reed and R. J. Gooding, *Phys. Rev. B* **50**, 3588 (1994); B. P. van Zyl and R. J. Gooding, <http://xxx.lanl.gov/archive/cond-mat/9602109>.
 - [4] *Metals Handbook*, 9th Edition, Vol. 4 (ASM, Ohio, 1981).
 - [5] M. Rao and S. Sengupta, *Phys. Rev. Lett.* **78**, 2168 (1997).